SIAM J. APPL. MATH.
Vol. 65, No. 5, pp. 1726–1747

NÉEL WALLS IN LOW ANISOTROPY SYMMETRIC DOUBLE LAYERS*

CARLOS J. GARCIA-CERVERA†

Abstract. A new model for the study of one-dimensional walls in magnetic multilayers is presented. We obtain the optimal scaling of this energy functional for low anisotropy double layers with magnetic layers of equal thickness. We prove that the optimal scaling may be attained by opposing Néel walls. We obtain the core length of the Néel wall and a detailed description of its structure. We illustrate our findings numerically.

Key words. micromagnetics, Landau–Lifshitz, Γ-limit, Néel walls

AMS subject classifications. 34B15, 34B60, 34E05, 49S05, 49K30, 65D99

DOI. 10.1137/S003613990343776X

1. Introduction.

A magnetic multilayer consists of two or more magnetic films, separated by a layer of nonmagnetic material (see Figure 1). Each layer may be of a different thickness. Multilayers seem to have good permanent magnet properties, in particular a high coercive field and approximately rectangular hysteresis loop [17]. For that reason multilayers are an integral part of magnetic memories (MRAMs) and have been one of the most important applications of ferromagnetic thin films in the past few years.

The magnetization distribution in a ferromagnetic material is described by the micromagnetics model, introduced by Landau and Lifshitz [12]. In nondimensional variables, the Landau–Lifshitz energy functional for a sample occupying a volume V is

$$F[\mathbf{m}] = \frac{q}{2}\int_V \Phi(\mathbf{m})\,dx + \frac{1}{2}\int_V |\nabla \mathbf{m}|^2\,dx + \frac{1}{2}\int_{\mathbb{R}^3} |\nabla \eta|^2\,dx. \tag{1.1}$$

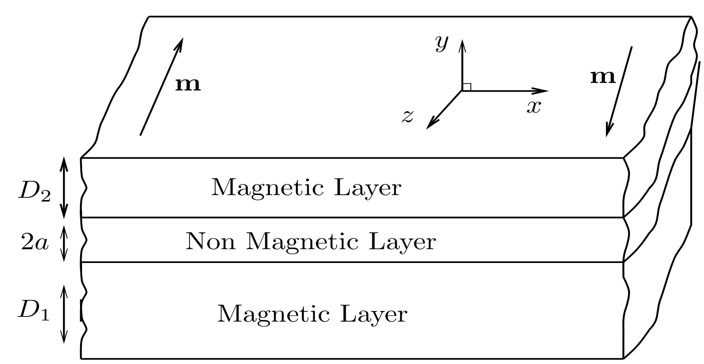

FIG. 1. *One-dimensional wall setting in a multilayer.*

*Received by the editors November 18, 2003; accepted for publication (in revised form) January 3, 2005; published electronically July 26, 2005.
http://www.siam.org/journals/siap/65-5/43776.html

†Mathematics Department, University of California, Santa Barbara, CA 93106 (cgarcia@math.ucsb.edu, http://www.math.ucsb.edu/∼cgarcia).

In (1.1), $|\mathbf{m}| = 1$ in V, and $\mathbf{m} = 0$ outside V. The three terms in (1.1) are anisotropy, exchange, and stray field energy, respectively. The parameter q is the quality factor, defined as $q = K_u/(\mu_0 M_s^2)$, where K_u is the crystalline anisotropy constant, M_s is the saturation magnetization, and μ_0 is the permeability of vacuum ($\mu_0 = 4\pi \times 10^{-7} N/A^2$). In (1.1), lengths are measured in units of the exchange length, $l = \sqrt{C_{ex}/(\mu_0 M_s^2)}$, where C_{ex} is the exchange constant. The energy is measured in units of $e = \sqrt{\mu_0 M_s^2 C_{ex}}$.

The stray field is $\mathbf{h}_s = -\nabla\eta$, where η is obtained by solving the equation

$$\text{div } (-\nabla\eta + \mathbf{m}) = 0 \quad \text{in } \mathbb{R}^3 \tag{1.2}$$

in the sense of distributions. The solution has the explicit form

$$\eta = \nabla N * \mathbf{m}, \tag{1.3}$$

where $N(\mathbf{x}) = -\frac{1}{4\pi}\frac{1}{|\mathbf{x}|}$ is the Newtonian potential.

For physical parameters typical of Permalloy ($C_{ex} = 1.3 \times 10^{-11} J/m$, $K_u = 5 \times 10^2 J/m^3$, $M_s = 8 \times 10^5 A/m$), the quality factor is $q \approx 6.21 \times 10^{-3}$. Thus it is physically relevant to consider the low anisotropy limit $q \to 0$, which is the situation considered in this article.

Functional (1.1) has been the focus of recent attention in the mathematical community, and the energy landscape for a single magnetic layer is now fairly well understood [9, 4, 5, 6, 8, 7, 18].

Due to the nonlocal nature of the magnetostatic interactions, the behavior of the magnetization distribution in double layers is very different from the single layer case. The magnetization patterns correspond to local minimizers of the Landau–Lifshitz energy. In a double layer, a pattern that would otherwise be energetically unfavorable for a single layer can be permitted by producing a pattern in the other layer which will cause the necessary field cancellations. With this compensating mechanism, new phenomena occur that are intrinsic to double layers.

The domain structure in magnetic films can be rather complicated [10, 6, 18]. In order to understand the structure in double films, we start by analyzing one-dimensional profiles, which will be the building blocks of more complicated structures. We are interested in both the structure and the energy of the minimizers. We are mainly interested in the scaling of the energy in terms of q as $q \to 0$, since all other parameters are kept fixed. To determine the energy of the minimizers, we consider an appropriate function in the admissible class, which provides us with an upper bound for the energy in terms of q. Subsequently we find a lower bound for the energy with the same scaling in q. The upper bound and the matching lower bound ensure that the energy is optimal, at least in terms of scaling.

In this article, we focus on the study of Néel walls in multilayers formed by two layers of equal thickness. Throughout this article we will refer to these multilayers as symmetric double layers. A description of the Néel wall in a single ferromagnetic layer was presented in [7], where the following energy functional, due originally to Aharoni [1], was analyzed:

$$\begin{aligned} F_{q,\delta}^A[\mathbf{m}] = \frac{q}{2}\int_{\mathbb{R}} \left(m_1^2 + m_2^2\right) + \frac{1}{2}\int_{\mathbb{R}} |\mathbf{m}'|^2 + \frac{1}{2}\int_{\mathbb{R}} \left(m_1^2 - m_1\left(\Gamma_\delta * m_1\right)\right) \\ + \frac{1}{2}\int_{\mathbb{R}} m_2\left(\Gamma_\delta * m_2\right). \end{aligned} \tag{1.4}$$

The set of admissible functions is

$$
\mathcal{A} = \Big\{ \mathbf{m} = (m_1, m_2, m_3) | m_1, m_2 \in H^1(\mathbb{R}),\ m_3' \in L^2(\mathbb{R}),\ |\mathbf{m}| = 1 \text{ a.e.}, \\ \mathbf{m} \to \pm \mathbf{e}_3 \text{ as } x \to \pm\infty \Big\}. \tag{1.5}
$$

In (1.4), δ represents the (rescaled) thickness of the sample, and

$$
\Gamma_\delta(x) = \frac{1}{4\pi\delta} \log\left(1 + \frac{4\delta^2}{x^2}\right). \tag{1.6}
$$

Functional (1.4) is derived directly from (1.1) by considering magnetization profiles that depend only on the x-variable. Functional (1.4) provides an accurate description of the minimizers for thin films ($\delta \ll 1$), since the dependence on the thickness variable becomes negligible as $\delta \to 0$ [9, 6, 8, 7, 18, 11, 3]. For thicker films, lower energy can be achieved with higher-dimensional structures [10, 18, 16].

For the study of Néel walls, we consider magnetization profiles such that $m_2 = 0$. The optimal energy scaling for a Néel wall in a single layer was obtained in [7]. In particular, it was proved that for a given $\delta > 0$ there exist positive constants c_0 and C_0 such that

$$
\frac{c_0}{\log \frac{1}{q}} \le \inf_{\mathbf{m} \in \mathcal{A}, m_2 = 0} F^A_{q,\delta}[\mathbf{m}] \le \frac{C_0}{\log \frac{1}{q}} \tag{1.7}
$$

as $q \to 0$. Moreover, it was shown that the Néel wall has a long logarithmic tail, which extends the stray field interactions to great distances.

In double layers the structure of Néel walls can be very different [14, 19, 20]. In this article we prove that in low anisotropy symmetric double layers, the logarithmic tail of the Néel wall disappears. The stray field becomes an exchange-type energy, and the wall becomes more localized and similar to the Landau–Lifshitz wall [12].

Considering a double layer as depicted in Figure 1, we have derived the following one-dimensional model for the study of magnetic walls in double layers:

$$
\begin{aligned}
G_{q,\alpha,\delta_1,\delta_2}[\mathbf{m}_1, \mathbf{m}_2] = {} & F_{q,\delta_1}[\mathbf{m}_1] + \frac{\delta_2}{\delta_1} F_{q,\delta_2}[\mathbf{m}_2] \\
& + \frac{\delta_2}{2} \int_{\mathbb{R}} u_1 \left(u_2 * \Theta_{\alpha,\delta_1,\delta_2}\right) - v_1 \left(v_2 * \Theta_{\alpha,\delta_1,\delta_2}\right) dx \\
& + \frac{\delta_2}{2} \int_{\mathbb{R}} v_1 \left(u_2 * \Psi_{\alpha,\delta_1,\delta_2}\right) - u_1 \left(v_2 * \Psi_{\alpha,\delta_1,\delta_2}\right) dx,
\end{aligned} \tag{1.8}
$$

where $\mathbf{m}_1 = (u_1, v_1, w_1)$ and $\mathbf{m}_2 = (u_2, v_2, w_2)$ represent the magnetization inside each layer, F_{q,δ_1} and F_{q,δ_2} are as in (1.4), and

$$
\begin{aligned}
\Theta_{\alpha,\delta_1,\delta_2}(x) &= \frac{1}{2\delta_1\delta_2\pi} \left(\log\left(\frac{x^2 + (2\alpha+\delta_1)^2}{x^2 + (2\alpha+\delta_1+\delta_2)^2} \right) - \log\left(\frac{x^2 + 4\alpha^2}{x^2 + (2\alpha+\delta_2)^2} \right) \right), \\
\Psi_{\alpha,\delta_1,\delta_2}(x) &= \frac{1}{\delta_1\delta_2\pi} \left(\arctan\left(\frac{2\alpha+\delta_1}{x-s} \right) - \arctan\left(\frac{2\alpha}{x-s} \right) \right. \\
& \qquad \left. - \arctan\left(\frac{2\alpha+\delta_1+\delta_2}{x-s} \right) + \arctan\left(\frac{2\alpha+\delta_2}{x-s} \right) \right).
\end{aligned} \tag{1.9}
$$

We have not been able to find this model in the literature, and therefore a complete derivation of this model is given in Appendix A. For the study of Néel walls, we assume $v_1 = v_2 = 0$. For a symmetric double layer, $\delta_1 = \delta_2 = \delta$.

This article is organized as follows. In section 2, we obtain the optimal energy scaling for Néel walls in symmetric double layers. In particular, we show that for fixed $\delta > 0$ and $\alpha > 0$ there exists a constant $C_0 > 0$ such that

$$4\sqrt{q} \leq \inf_{\mathbf{m}\in\mathcal{A}} G_{q,\alpha,\delta,\delta}[\mathbf{m}] \leq C_0\sqrt{q}. \tag{1.10}$$

The upper bound is obtained considering Néel walls in the double layer.

A more detailed analysis is carried out in section 3, where we prove that for a family of minimizers of the Néel wall functional (2.7), $\{\mathbf{m}_q\}_{\{q>0\}}$,

(1.11)
$$\lim_{q\to 0} \frac{1}{\sqrt{q}} G_{q,\alpha,\delta,\delta}[\mathbf{m}_q] = \min_{\mathbf{m}\in\mathcal{A}, m_2=0} \int_{\mathbb{R}} m_1^2\,dx + \frac{\delta\,(\delta+3\alpha)}{3}\int_{\mathbb{R}} (m_1')^2\,dx + \int_{\mathbb{R}} |\mathbf{m}'|^2\,dx.$$

We also prove that, given a family of minimizers $\{\mathbf{m}_q\}_{\{q>0\}}$, we can extract a sequence (not relabeled) such that the rescaled family $\{\mathbf{m}_q(x/\sqrt{q})\}_{\{q>0\}}$ converges strongly in $H^1(\mathbb{R})$. We interpret this in the Γ-limit sense of an appropriately scaled family of functionals. The limiting profile is studied in section 4 using a formal asymptotic expansion.

In section 5 we illustrate all of our findings numerically. To this end, we have implemented a modified Newton method for energy minimization. Finally, a detailed derivation of the model used in this article is presented in Appendix A.

2. Optimal scaling: Opposing Néel walls. Since the stray field energy is nonnegative, the Landau–Lifshitz wall profile always provides us with a lower bound for the energy:

$$G_{q,\alpha,\delta}[\mathbf{m}_1,\mathbf{m}_2] \geq \min_{\mathbf{m}_1,\mathbf{m}_2\in\mathcal{A}} \widetilde{F}_q[\mathbf{m}_1,\mathbf{m}_2], \tag{2.1}$$

where

$$\widetilde{F}_q[\mathbf{m}_1,\mathbf{m}_2] = \frac{1}{2}\sum_{j=1}^{2}\left(q\int_{\mathbb{R}}(u_j^2+v_j^2)\,dx + \int_{\mathbb{R}}|\mathbf{m}_j'|^2\,dx\right). \tag{2.2}$$

Since $\mathbf{m}_1$ and $\mathbf{m}_2$ are decoupled in (2.2), the minimum will be achieved for $\mathbf{m}_1 = \mathbf{m}_2 = (u,v,w)$. Moreover, we can assume that either $u=0$ or $v=0$. Otherwise, following Lemma 4 in [7], consider $\widetilde{\mathbf{m}} = (\sqrt{u^2+v^2},0,w)$. Then

$$\begin{aligned}\widetilde{F}_q[\widetilde{\mathbf{m}},\widetilde{\mathbf{m}}] &= q\int_{\mathbb{R}}(u^2+v^2) + \int_{\mathbb{R}}\left(\frac{(uu'+vv')^2}{u^2+v^2} + (w')^2\right)\\ &= q\int_{\mathbb{R}}(u^2+v^2) + \int_{\mathbb{R}}|\mathbf{m}'|^2 - \int_{\mathbb{R}}\frac{(uv'-vu')^2}{u^2+v^2} \leq \widetilde{F}_q[\mathbf{m},\mathbf{m}].\end{aligned} \tag{2.3}$$

Therefore, a lower bound for (1.8) in a symmetric double layer is obtained by minimizing

$$\min_{\mathbf{m}\in\mathcal{A},m_2=0} \widetilde{F}_q[\mathbf{m},\mathbf{m}]. \tag{2.4}$$

This is the minimization problem studied by Landau and Lifshitz in [12]. The minimizer is

$$\mathbf{m} = (\operatorname{sech}(\sqrt{q}x), 0, \tanh(\sqrt{q}x)), \tag{2.5}$$

and the minimum energy is

$$q\int_{\mathbb{R}} u^2\,dx + \int_{\mathbb{R}} |\mathbf{m}'|^2\,dx = 4\sqrt{q}. \tag{2.6}$$

In a single layer, this is not optimal for a Néel wall, as proved in [7]. However, we can prove that, due to stray field cancellations, this energy scaling is indeed optimal in a symmetric double layer.

To obtain a matching upper bound for the energy, we consider Néel walls in symmetric double layers and study the functional

$$\begin{aligned} G_{q,\alpha,\delta}[\mathbf{m}_1,\mathbf{m}_2] = {}& \frac{q}{2}\int_{\mathbb{R}} u_1^2 + \frac{1}{2}\int_{\mathbb{R}} |\mathbf{m}_1'|^2 + \frac{1}{2}\int_{\mathbb{R}} \big(u_1^2 - u_1\,(\Gamma_\delta * u_1)\big) + \frac{q}{2}\int_{\mathbb{R}} u_2^2 \\ &+ \frac{1}{2}\int_{\mathbb{R}} |\mathbf{m}_2'|^2 + \frac{1}{2}\int_{\mathbb{R}} \big(u_2^2 - u_2\,(\Gamma_\delta * u_2)\big) + \frac{\delta}{2}\int_{\mathbb{R}} u_1\,(u_2 * \Theta_{\alpha,\delta}). \end{aligned} \tag{2.7}$$

In (2.13), we have renamed the energy functional $G_{q,\alpha,\delta} \equiv G_{q,\alpha,\delta,\delta}$, and the convolution kernel $\Theta_{\alpha,\delta} \equiv \Theta_{\alpha,\delta,\delta}$, in view of definitions (1.8) and (1.9), respectively. In Fourier space,

$$\begin{aligned} &G_{q,\alpha,\delta}[\mathbf{m}_1,\mathbf{m}_2] = \frac{q}{2}\int_{\mathbb{R}} |\widehat{u}_1|^2\,d\xi + \frac{1}{2}\int_{\mathbb{R}} 4\pi^2\xi^2|\widehat{\mathbf{m}}_1|^2\,d\xi + \frac{1}{2}\int_{\mathbb{R}} |\widehat{u}_1|^2\left(1-\widehat{\Gamma}_\delta(\xi)\right)d\xi \\ &+\frac{q}{2}\int_{\mathbb{R}} |\widehat{u}_2|^2\,d\xi + \frac{1}{2}\int_{\mathbb{R}} 4\pi^2\xi^2|\widehat{\mathbf{m}}_2|^2\,d\xi + \frac{1}{2}\int_{\mathbb{R}} |\widehat{u}_2|^2\left(1-\widehat{\Gamma}_\delta(\xi)\right)d\xi + \frac{\delta}{2}\Re\int_{\mathbb{R}} \widehat{u}_1\overline{\widehat{u}_2}\widehat{\Theta}_{a,\delta}(\xi)\,d\xi. \end{aligned} \tag{2.8}$$

In the following lemma, we prove that in a symmetric double layer the minimum of (2.7) is achieved by opposing Néel walls; i.e., $u_1 = -u_2$.

LEMMA 2.1. *Consider* $\mathbf{m}_1, \mathbf{m}_2 \in \mathcal{A}$, *where* $\mathbf{m}_1 = (u_1, 0, w_1)$ *and* $\mathbf{m}_2 = (u_2, 0, w_2)$. *Define* $\widetilde{\mathbf{m}}_1 = (-u_1, 0, w_1)$ *and* $\widetilde{\mathbf{m}}_2 = (-u_2, 0, w_2)$. *Then, either*

$$G_{q,\alpha,\delta}[\mathbf{m}_1, \widetilde{\mathbf{m}}_1] \le G_{q,\alpha,\delta}[\mathbf{m}_1, \mathbf{m}_2] \tag{2.9}$$

or

$$G_{q,\alpha,\delta}[\mathbf{m}_2, \widetilde{\mathbf{m}}_2] \le G_{q,\alpha,\delta}[\mathbf{m}_1, \mathbf{m}_2]. \tag{2.10}$$

Proof. We can rewrite the Fourier representation (2.8) as

$$\begin{aligned} G_{q,\alpha,\delta}[\mathbf{m}_1,\mathbf{m}_2] = {}& \frac{q}{2}\int_{\mathbb{R}} |\widehat{u}_1|^2\,d\xi + \frac{1}{2}\int_{\mathbb{R}} 4\pi^2\xi^2|\widehat{\mathbf{m}}_1|^2\,d\xi \\ &+ \frac{1}{2}\int_{\mathbb{R}} |\widehat{u}_1|^2\left(1-\widehat{\Gamma}_\delta(\xi) - \frac{\delta}{2}\widehat{\Theta}_{\alpha,\delta}(\xi)\right)d\xi + \frac{q}{2}\int_{\mathbb{R}} |\widehat{u}_2|^2\,d\xi + \frac{1}{2}\int_{\mathbb{R}} 4\pi^2\xi^2|\widehat{\mathbf{m}}_2|^2\,d\xi \\ &+ \frac{1}{2}\int_{\mathbb{R}} |\widehat{u}_2|^2\left(1-\widehat{\Gamma}_\delta(\xi) - \frac{\delta}{2}\widehat{\Theta}_{\alpha,\delta}(\xi)\right)d\xi + \frac{\delta}{4}\int_{\mathbb{R}} |\widehat{u}_1 + \widehat{u}_2|^2\widehat{\Theta}_{a,\delta}(\xi)\,d\xi. \end{aligned} \tag{2.11}$$

Note that

$$\int_{\mathbb{R}} |\widehat{u}_2|^2 \left(1 - \widehat{\Gamma}_\delta(\xi) - \frac{\delta}{2}\widehat{\Theta}_{\alpha,\delta}(\xi)\right) d\xi \tag{2.12}$$

is the stray field energy that corresponds to a symmetric double layer where $u_1 = -u_2$, and therefore it is nonnegative. Thus, given $(\mathbf{m}_1, \mathbf{m}_2)$, since all the terms in (2.11) are nonnegative, we can always lower the total energy by selecting $(\mathbf{m}_1, \widetilde{\mathbf{m}}_1)$ or $(\mathbf{m}_2, \widetilde{\mathbf{m}}_2)$. ◻

In view of this lemma, we need to consider only opposing Néel walls. Thus, we need to study functional

$$\begin{aligned}\widetilde{G}_{q,\alpha,\delta}[\mathbf{m}] = q\int_{\mathbb{R}} u^2\,dx + \int_{\mathbb{R}} |\mathbf{m}'|^2\,dx + \int_{\mathbb{R}} u^2\,dx - \int_{\mathbb{R}} u\,(\Gamma_\delta * u)\,dx \\ -\frac{\delta}{2}\int_{\mathbb{R}} u\,(u * \Theta_{\alpha,\delta})\,dx,\end{aligned} \tag{2.13}$$

which can be written in Fourier space as

$$\widetilde{G}_{q,\alpha,\delta}[\mathbf{m}] = q\int_{\mathbb{R}} |\widehat{u}|^2\,d\xi + \int_{\mathbb{R}} 4\pi^2\xi^2 |\widehat{\mathbf{m}}|^2\,d\xi + \int_{\mathbb{R}} |\widehat{u}|^2 \left(1 - \widehat{\Gamma}_\delta(\xi) - \frac{\delta}{2}\widehat{\Theta}_{\alpha,\delta}(\xi)\right) d\xi. \tag{2.14}$$

The lower semicontinuity and existence of minimizers of functional (2.13) follow from Lemmas 1, 2, and 3 in [7]. The main difficulty in establishing the existence of minimizers lies in the fact that functional (2.13) is translation invariant. This problem is resolved in [7] by considering a translation of $\mathbf{m}$ such that $\mathbf{m}(0) = (1, 0, 0)$. The result then follows from the Sobolev embedding and the Rellich compactness theorem [21].

As a consequence of Lemma 2.1,

$$\inf_{\mathbf{m}_1,\mathbf{m}_2\in\mathcal{A}} G_{q,\alpha,\delta}[\mathbf{m}_1, \mathbf{m}_2] = \inf_{\mathbf{m}\in\mathcal{A}} \widetilde{G}_{q,\alpha,\delta}[\mathbf{m}]. \tag{2.15}$$

Thus, the existence of minimizers for functional (2.7) is established. To simplify notation, in what follows we will drop the tilde from functional (2.13).

The matching upper bound that we need can be obtained by considering the test function $\mathbf{m} = (\operatorname{sech}(\sqrt{q}x), 0, \tanh(\sqrt{q}x))$, which is the Landau–Lifshitz wall. The Fourier transform of $u(x) = \operatorname{sech}(\sqrt{q}x)$ can be obtained by residues [2]:

$$\widehat{u}(\xi) = \frac{\pi}{\sqrt{q}}\operatorname{sech}\left(\frac{\pi^2\xi}{\sqrt{q}}\right). \tag{2.16}$$

The stray field energy of this profile is

$$\begin{aligned} E_s &= \int_{\mathbb{R}} \widehat{u}^2 \left(1 - \frac{1 - e^{-2\pi\delta|\xi|}}{2\pi\delta|\xi|} - \frac{1}{2}e^{-4\pi a|\xi|}\frac{(1 - e^{-2\pi\delta|\xi|})^2}{2\pi\delta|\xi|}\right) d\xi \\ &= \frac{\pi^2}{q}\int_{\mathbb{R}} \operatorname{sech}^2\left(\frac{\pi^2\xi}{\sqrt{q}}\right)\left(1 - \frac{1 - e^{-2\pi\delta|\xi|}}{2\pi\delta|\xi|} - \frac{1}{2}e^{-4\pi\alpha|\xi|}\frac{(1 - e^{-2\pi\delta|\xi|})^2}{2\pi\delta|\xi|}\right) d\xi \\ &= \frac{1}{\sqrt{q}}\int_{\mathbb{R}} \operatorname{sech}^2(\xi)\left(1 - \frac{1 - e^{-2\delta|\xi|\sqrt{q}/\pi}}{2\delta|\xi|\sqrt{q}/\pi} - \frac{1}{2}e^{-4\alpha|\xi|\sqrt{q}/\pi}\frac{(1 - e^{-2\delta|\xi|\sqrt{q}/\pi})^2}{2\delta|\xi|\sqrt{q}/\pi}\right) d\xi \\ &= \frac{4\delta\sqrt{q}}{\pi^2}\left(\frac{\delta}{3} + \alpha\right)\int_{\mathbb{R}} |\xi|^2 \operatorname{sech}^2(\xi)\,d\xi + O(q) = \frac{2\delta\sqrt{q}}{3}\left(\frac{\delta}{3} + \alpha\right) + O(q). \end{aligned} \tag{2.17}$$

Therefore $\exists q_0 > 0$ such that

$$E_s \le \frac{4\delta\sqrt{q}}{3}\left(\frac{\delta}{3}+\alpha\right) \quad \forall q \le q_0. \tag{2.18}$$

The total energy is therefore

$$\widetilde{G}_{q,\alpha,\delta}[\mathbf{m}] = \left\{4+\frac{2\delta}{3}\left(\frac{\delta}{3}+\alpha\right)\right\}\sqrt{q}+O(q) \le 4\left\{1+\frac{\delta}{3}\left(\frac{\delta}{3}+\alpha\right)\right\}\sqrt{q} \quad \forall q \le q_0. \tag{2.19}$$

We collect all this in the following theorem.

THEOREM 2.2. *Consider the one-dimensional wall energy functional for a symmetric double layer* (1.8). *Given $\alpha > 0$ and $\delta > 0$ fixed, $\exists\ q_0 > 0$ such that*

$$4\sqrt{q} \le \min_{\mathbf{m}_1,\mathbf{m}_2\in\mathcal{A}} G_{q,\alpha,\delta,\delta}[\mathbf{m}_1,\mathbf{m}_2] \le 4\left\{1+\frac{\delta}{3}\left(\frac{\delta}{3}+\alpha\right)\right\}\sqrt{q} \quad \forall q \le q_0. \tag{2.20}$$

An estimate of the value of q_0 is presented in Appendix B.

3. Néel walls: Limiting behavior. In this section we study the structure of Néel walls in symmetric double layers and obtain the limiting behavior of any sequence of minimizers of the Néel wall functional (2.13). This is the content of the following theorem.

THEOREM 3.1. *Given $\alpha > 0$ and $\delta > 0$, consider $\{\mathbf{m}_q\}_{\{q>0\}} \subset \mathcal{A}_N = \{\mathbf{m} = (m_1, 0, m_3) \in \mathcal{A}\}$ such that*

$$G_{q,\alpha,\delta}[\mathbf{m}_q] \le C\sqrt{q}, \tag{3.1}$$

and define $\widetilde{\mathbf{m}}_q(x) = \mathbf{m}_q(\frac{x}{\sqrt{q}})$. There exists a subsequence of $\{\mathbf{m}_q\}_{\{q>0\}}$ (not relabeled) such that the following two statements hold:

(i)

$$\lim_{q\to 0}\frac{1}{\sqrt{q}}G_{q,\alpha,\delta}[\mathbf{m}_q] = \min_{\mathbf{m}\in\mathcal{A}_N} F_{\alpha,\delta}[\mathbf{m}], \tag{3.2}$$

where

$$F_{\alpha,\delta}[\mathbf{m}] = \int_{\mathbb{R}} m_1^2\,dx + \left(1+\delta\left(\frac{1}{3}\delta+\alpha\right)\right)\int_{\mathbb{R}}(m_1')^2\,dx + \int_{\mathbb{R}}(m_3')^2\,dx. \tag{3.3}$$

(ii) *The subsequence converges strongly in $\mathcal{A}_N$ to $\mathbf{n} \in \mathcal{A}_N$ such that*

$$F_{\alpha,\delta}[\mathbf{n}] = \min_{\mathbf{m}\in\mathcal{A}_N} F_{\alpha,\delta}[\mathbf{m}]. \tag{3.4}$$

Proof. Given the sequence of minimizers, consider the new rescaled sequence $\widetilde{\mathbf{m}}_q(x) = \mathbf{m}_q(\frac{x}{\sqrt{q}})$. This sequence is bounded in the following sense:

$$\begin{aligned}\int_{\mathbb{R}}\widetilde{u}_q^2(x)\,dx + \int_{\mathbb{R}}|\widetilde{\mathbf{m}}_q'|^2\,dx &= \sqrt{q}\int_{\mathbb{R}}u_q^2(x)\,dx + \frac{1}{\sqrt{q}}\int_{\mathbb{R}}|\mathbf{m}_q'|^2\,dx \\ &\le \frac{1}{\sqrt{q}}G_{q,\alpha,\delta}[\mathbf{m}_q] \le C.\end{aligned} \tag{3.5}$$

Thus there is a subsequence (not relabeled) that converges weakly in $\mathcal{A}_N$ to $\mathbf{n} \in \mathcal{A}_N$.

Consider now $\mathbf{n}_q(x) = \mathbf{n}(\sqrt{q}x)$. Then,

$$\widehat{\mathbf{n}}_q(\xi) = \frac{1}{\sqrt{q}}\widehat{\mathbf{n}}\left(\frac{\xi}{\sqrt{q}}\right) \tag{3.6}$$

and

$$\begin{aligned} G_{q,\alpha,\delta}[\mathbf{n}_q] &= \sqrt{q}\int_{\mathbb{R}} u^2(\xi)\,d\xi + \sqrt{q}\int_{\mathbb{R}} 4\pi^2\xi^2|\widehat{\mathbf{n}}(\xi)|^2\,d\xi \\ &+ \frac{1}{\sqrt{q}}\int_{\mathbb{R}} \widehat{u}^2(\xi)\left(1 - \frac{1-e^{-2\pi\delta|\xi|\sqrt{q}}}{2\pi\delta|\xi|\sqrt{q}} - \frac{1}{2}e^{-4\pi a|\xi|\sqrt{q}}\frac{(1-e^{-2\pi\delta|\xi|\sqrt{q}})^2}{2\pi\delta|\xi|\sqrt{q}}\right)d\xi. \end{aligned} \tag{3.7}$$

We need to take the limit of the stray field energy. Since $\alpha\sqrt{q} \ll 1$ and $\delta\sqrt{q} \ll 1$,

$$\lim_{q\to 0}\frac{1}{q}\left(1 - \frac{1-e^{-2\pi\delta|\xi|\sqrt{q}}}{2\pi\delta|\xi|\sqrt{q}} - \frac{1}{2}e^{-4\pi a|\xi|\sqrt{q}}\frac{(1-e^{-2\pi\delta|\xi|\sqrt{q}})^2}{2\pi\delta|\xi|\sqrt{q}}\right) = \left(\frac{1}{3}\delta + a\right)4\pi^2|\xi|^2\delta. \tag{3.8}$$

The stray field energy can be written as

$$\frac{1}{\sqrt{q}}E_s = \delta\left(\frac{1}{3}\delta + a\right)\int_{\mathbb{R}} 4\pi^2\xi^2\widehat{u}^2(\xi)\widehat{\varphi}(\sqrt{q}\xi)\,d\xi, \tag{3.9}$$

where

$$\widehat{\varphi}(\xi) = \frac{1}{\left(\frac{1}{3}\delta + a\right)}\frac{1}{4\pi^2\xi^2}\left(1 - \frac{1-e^{-2\pi\delta|\xi|}}{2\pi\delta|\xi|} - \frac{1}{2}e^{-4\pi a|\xi|}\frac{(1-e^{-2\pi\delta|\xi|})^2}{2\pi\delta|\xi|}\right). \tag{3.10}$$

Note that $\widehat{\varphi}(0) = 1$ and $\widehat{\varphi} \in L^1(\mathbb{R}) \cap L^\infty(\mathbb{R})$, so $\varphi \in L^1(\mathbb{R}) \cap L^2(\mathbb{R})$. Therefore, the stray field can be written, in real space, as

$$\frac{1}{\sqrt{q}}E_s = \delta\left(\frac{1}{3}\delta + a\right)\int_{\mathbb{R}} u\left(u * \varphi_{\sqrt{q}}\right)dx, \tag{3.11}$$

where $\varphi_{\sqrt{q}}(x) = \frac{1}{\sqrt{q}}\phi(\frac{x}{\sqrt{q}})$, which is an approximation to the identity. Therefore we can take the limit in (3.7), and we obtain

$$\begin{aligned} \lim_{q\to 0}\frac{1}{\sqrt{q}}G_{q,\alpha,\delta}[\mathbf{n}_q] &= \int_{\mathbb{R}} \widehat{u}^2(\xi)\,d\xi + \int_{\mathbb{R}} 4\pi^2\xi^2\left(1 + \delta\left(\frac{1}{3}\delta + a\right)\right)|\widehat{u}(\xi)|^2\,d\xi \\ &+ \frac{1}{2}\int_{\mathbb{R}} 4\pi^2\xi^2|\widehat{w}(\xi)|^2\,d\xi = \int_{\mathbb{R}} u^2\,dx + \left(1 + \delta\left(\frac{1}{3}\delta + a\right)\right)\int_{\mathbb{R}}(u')^2\,dx + \int_{\mathbb{R}}(w')^2\,dx \\ &= F_{\alpha,\delta}[\mathbf{n}]. \end{aligned} \tag{3.12}$$

Since $\mathbf{m}_q$ was a minimizer,

$$\frac{1}{\sqrt{q}}G_{q,\alpha,\delta}[\mathbf{m}_q] \le \frac{1}{\sqrt{q}}G_{q,\alpha,\delta}[\mathbf{n}_q], \tag{3.13}$$

and thus

$$\limsup_{q\to 0}\frac{1}{\sqrt{q}}G_{q,\alpha,\delta}[\mathbf{m}_q] \le \lim_{q\to 0}\frac{1}{\sqrt{q}}G_{q,\alpha,\delta}[\mathbf{n}_q] = F_{\alpha,\delta}[\mathbf{n}]. \tag{3.14}$$

Observe now that

$$\frac{1}{\sqrt{q}} G_{q,\alpha,\delta}[\mathbf{m}_q] = H_{q,\alpha,\delta}[\widetilde{\mathbf{m}}_q], \tag{3.15}$$

where

$$H_{q,\alpha,\delta}[\mathbf{m}] = \int_{\mathbb{R}} u^2\,dx + \int_{\mathbb{R}} |\mathbf{m}'|^2\,dx + \delta\left(\frac{1}{3}\delta + \alpha\right)\int_{\mathbb{R}} u\left(u * \varphi_{\sqrt{q}}\right)dx. \tag{3.16}$$

Since $\widetilde{\mathbf{m}}_q$ converges to $\mathbf{n}$ weakly in $\mathcal{A}_N$, by the lower semicontinuity of the functional,

$$F_{\alpha,\delta}[\mathbf{n}] \le \liminf_{q\to 0} \frac{1}{\sqrt{q}} G_{q,\alpha,\delta}[\mathbf{m}_q]. \tag{3.17}$$

Combining (3.14) and (3.17), we conclude that

$$\lim_{q\to 0} \frac{1}{\sqrt{q}} G_{q,\alpha,\delta}[\mathbf{m}_q] = F_{\alpha,\delta}[\mathbf{n}]. \tag{3.18}$$

It is easy to see that $\mathbf{n}$ must be a minimizer of $F_{\alpha,\delta}$: Given any $\mathbf{m}_0 \in \mathcal{A}$, consider $\widetilde{\mathbf{n}}_q(x) = \mathbf{m}_0\left(\sqrt{q}x\right)$. Then

$$F_{\alpha,\delta}[\mathbf{m}_0] = \lim_{q\to 0} \frac{1}{\sqrt{q}} G_{q,\alpha,\delta}[\widetilde{\mathbf{n}}_q] \ge \lim_{q\to 0} \frac{1}{\sqrt{q}} G_{q,\alpha,\delta}[\mathbf{m}_q] = F_{\alpha,\delta}[\mathbf{n}]. \tag{3.19}$$

This proves (i). Since the sequence $\mathbf{n}_q$ converges weakly to $\mathbf{n}$ and the energies converge, the limit is strong, which proves (ii). ∎

From the previous proof, it is easy to see that $H_{q,\alpha,\delta} \to F_{\alpha,\delta}$ in $\mathcal{A}_N$ as $q \to 0$, in the Γ-limit sense [13].

4. Asymptotic analysis of the limiting profile. We perform a formal asymptotic expansion of the minimizers of functional $F_{\alpha,\delta}$, defined in (3.3), for $\delta \ll 1$. Since $|\mathbf{m}| = 1$, it is customary to write $\mathbf{m} = (\cos\theta, 0, \sin\theta)$, where $\theta \to \pm\frac{\pi}{2}$ as $x \to \pm\infty$. We consider the functional

$$F_\beta[\mathbf{m}] = \int_{\mathbb{R}} m_1^2\,dx + (1+\beta)\int_{\mathbb{R}} (m_1')^2\,dx + \int_{\mathbb{R}} (m_3')^2\,dx, \tag{4.1}$$

where $\beta = \delta(3\alpha + \delta)/3 \ll 1$. We do the change of variables to θ, and get

$$F_\beta[\theta] = \int_{\mathbb{R}} \cos^2\theta\,dx + \int_{\mathbb{R}} (\theta')^2\,dx + \beta\int_{\mathbb{R}} (\theta')^2 \sin^2\theta\,dx. \tag{4.2}$$

The Euler–Lagrange equation is

$$(1 + \beta\sin^2\theta)\theta'' + (1 + \beta(\theta')^2)\sin\theta\cos\theta = 0. \tag{4.3}$$

For $\beta = 0$, we get

$$\theta'' + \sin\theta\cos\theta = 0, \tag{4.4}$$

which has as solution $\cos\theta = \tanh x$. This is the Landau–Lifshitz profile [12]. The asymptotic analysis can be carried out more easily if we consider profiles of the form

$\mathbf{m} = (\operatorname{sech}\varphi, 0, \tanh\varphi)$ instead, and write the equation for φ. Since $\cos\theta = \operatorname{sech}\varphi$ and $\sin\theta = \tanh\varphi$, we get $\theta' = \varphi' \operatorname{sech}\varphi$ and

$$\theta'' = \operatorname{sech}\varphi \left(\varphi'' - (\varphi')^2 \tanh\varphi\right). \tag{4.5}$$

The equation becomes then

$$\left(1 + \beta \tanh^2\varphi\right)\left(\varphi'' - (\varphi')^2 \tanh\varphi\right) + \left(1 + \beta(\varphi')^2 \operatorname{sech}^2\varphi\right)\tanh\varphi = 0. \tag{4.6}$$

Assume that $\varphi \sim \varphi_0 + \beta\varphi_1 + O(\beta^2)$. Then,

$$\begin{aligned}&\left(1 + \beta \tanh^2(\varphi_0 + \beta\varphi_1)\right)\left(\varphi_0'' + \beta\varphi_1'' - (\varphi_0' + \beta\varphi_1')^2 \tanh(\varphi_0 + \beta\varphi_1)\right)\\ &\quad + \left(1 + \beta(\varphi_0' + \beta\varphi_1')^2 \operatorname{sech}^2(\varphi_0 + \beta\varphi_1)\right)\tanh(\varphi_0 + \beta\varphi_1) = 0.\end{aligned} \tag{4.7}$$

Collecting terms, we get

$$\varphi_0'' + (1 - (\varphi_0')^2)\tanh\varphi_0 = 0. \tag{4.8}$$

The solution is $\varphi_0 = x$. The next term in (4.7) is

$$\begin{aligned}&\varphi_1'' - 2\varphi_1'\varphi_0' \tanh\varphi_0 - (\varphi_0')^2 \operatorname{sech}^2\varphi_0\varphi_1 + \tanh^2(\varphi_0)\left(\varphi_0'' - (\varphi_0')^2 \tanh\varphi_0\right)\\ &\quad + (\varphi_0')^2 \operatorname{sech}^2\varphi_0 \tanh\varphi_0 + \operatorname{sech}^2\varphi_0\varphi_1 = 0.\end{aligned} \tag{4.9}$$

Since $\varphi_0 = x$ and $\varphi_0' = 1$, the equation simplifies to

$$\varphi_1'' - 2\varphi_1' \tanh x - \tanh^3 x + \operatorname{sech}^2 x \tanh x = 0. \tag{4.10}$$

Then

$$\left(\frac{\varphi_1'}{\cosh^2 x}\right)' = \frac{\varphi_1'' - 2\varphi_1' \tanh x}{\cosh^2 x} = \operatorname{sech}^2 x \tanh^3 x - \operatorname{sech}^4 x \tanh x. \tag{4.11}$$

We can integrate the right-hand side:

$$\begin{aligned}\int \operatorname{sech}^2 x \tanh^3 x\, dx &= \int \frac{\sinh x\left(\cosh^2 x - 1\right)}{\cosh^5 x}\, dx = \frac{1}{4}\frac{1}{\cosh^4 x} - \frac{1}{2}\frac{1}{\cosh^2 x},\\ \int \operatorname{sech}^4 x \tanh x\, dx &= \int \frac{\sinh x}{\cosh^5 x}\, dx = -\frac{1}{4}\frac{1}{\cosh^4 x}.\end{aligned} \tag{4.12}$$

Therefore,

$$\varphi_1' = C\cosh^2 x + \frac{1}{2}\frac{1}{\cosh^2 x} - \frac{1}{2} \tag{4.13}$$

and, integrating,

$$\varphi_1 = C\frac{\sinh 2x + 2x}{4} + \frac{1}{2}\tanh x - \frac{x}{2} + D. \tag{4.14}$$

We want φ to be odd, so $D = 0$. Unless $C = 0$, φ_1 will dominate over φ_0, so we take $C = 0$, and finally,

$$\varphi_1 = \frac{1}{2}\tanh x - \frac{x}{2}. \tag{4.15}$$

Therefore,

$$\mathbf{m} = \left(\operatorname{sech}\left(x + \frac{\beta}{2}(\tanh x - x)\right), 0, \tanh\left(x + \frac{\beta}{2}(\tanh x - x)\right)\right) + O(\beta^2). \tag{4.16}$$

5. Numerical experiments. We have implemented a truncated Newton method with an inexact line search for the minimization of

$$\begin{aligned} G_{q,\alpha,\delta}[\mathbf{m}_1,\mathbf{m}_2] = \frac{1}{2}q\int_{\mathbb{R}} u_1^2\,dx + \frac{1}{2}\int_{\mathbb{R}} |\mathbf{m}_1'|^2\,dx + \frac{1}{2}\int_{\mathbb{R}} u_1^2\,dx - \frac{1}{2}\int_{\mathbb{R}} u_1\,(\Gamma_\delta * u_1)\,dx \\ + \frac{1}{2}q\int_{\mathbb{R}} u_2^2\,dx + \frac{1}{2}\int_{\mathbb{R}} |\mathbf{m}_2'|^2\,dx + \frac{1}{2}\int_{\mathbb{R}} u_2^2\,dx - \frac{1}{2}\int_{\mathbb{R}} u_2\,(\Gamma_\delta * u_2)\,dx \\ - \frac{\delta}{2}\int_{\mathbb{R}} u_1\,(u_2 * \Theta_{\alpha,\delta})\,dx. \end{aligned} \tag{5.1}$$

The method is well known, and the details can be found in the literature [15], so we will simply describe some of the details particular to our implementation.

We consider a finite interval $I = [-M, M]$, and restrict the functional to I. We have performed simulations in several intervals of increasing size until no change was found in the characteristics of the wall. For the results presented here we used $I = [-200, 200]$. We define the grid points $x_i = -M + i\Delta x$, for $i = 0, 1, \dots, n+1$, where $\Delta x = \frac{2M}{n+1}$. The magnetization is approximated by a linear interpolant in the subinterval $I_i = [x_i, x_{i+1}]$, for $i = 0, 1, \dots, n$. We impose the boundary conditions $u_0 = u_{n+1} = 0$. For the simulations presented here we fixed the parameters $\delta = 1$ and $a = 10^{-1}$. The parameter q varied in the range $q \in [10^{-3}, 1]$.

To evaluate the stray field, we need to approximate convolution integrals of the form

$$v(x_j) = \int_{-M}^{M} u(s) K(x_j - s)\,ds. \tag{5.2}$$

Substituting the piecewise linear interpolant,

$$v(x_j) \approx \sum_{i=0}^{n} \int_{x_i}^{x_{i+1}} \left(u_i + \frac{u_{i+1} - u_i}{\Delta x}(s - x_i) \right) K(x_j - s)\,ds. \tag{5.3}$$

Grouping terms,

$$v_j = \sum_{i=1}^{n} u_i \left[\int_{x_i}^{x_{i+1}} \left(1 - \frac{(s - x_i)}{\Delta x} \right) K(x_j - s)\,ds + \int_{x_{i-1}}^{x_i} \frac{(s - x_{i-1})}{\Delta x} K(x_j - s)\,ds \right]. \tag{5.4}$$

This can be written in the form

$$v_j = \sum_{i=1}^{n} K_{j-i} u_i, \tag{5.5}$$

where

$$K_\lambda = \Delta x \int_0^1 (1 - t)\, K\left(\Delta x(\lambda - t)\right) + tK\left(\Delta x(\lambda + 1 - t)\right) dt. \tag{5.6}$$

The sum (5.5) has the shape of a discrete convolution, and it can therefore be efficiently evaluated using the fast Fourier transform (FFT) in $O(n \log n)$ operations.

The unit length constraint in the magnetization is taken into account by considering a line search on the function

$$h(\epsilon) = G_{q,\alpha,\delta}\left[\frac{\mathbf{m}_1+\epsilon\mathbf{p}_1}{|\mathbf{m}_1+\epsilon\mathbf{p}_1|}, \frac{\mathbf{m}_2+\epsilon\mathbf{p}_2}{|\mathbf{m}_2+\epsilon\mathbf{p}_2|}\right], \tag{5.7}$$

where $(\mathbf{p}_1, \mathbf{p}_2)$ is a descent direction, i.e., $h'(0) < 0$.

In Figure 2 we show the profiles of several minimizers as a function of q. All the numerically computed minimizers were opposed Néel walls, consistent with Lemma 2.1. These same profiles are presented in Figure 3, but this time the abscissa is rescaled by $\sqrt{q}$. As can be seen, all the plots collapse into one, illustrating that the core length is $1/\sqrt{q}$, as proved in section 4. This limiting profile is plotted in Figure 4, where it is compared to the profile of the minimizer of (5.1) computed numerically. The profiles are almost indistinguishable.

The computed values for the minimum energy as a function of q are presented in Table 1. From the results in the third column it is clear that the energy scales like $\sqrt{q}$. We plot the results in a logarithmic scale in Figure 5. The energy of the asymptotic approximation (4.16) was computed to machine precision using adaptive Gaussian quadrature. The computed energy coincides to a remarkable degree with the energy obtained using the asymptotic analysis described in the previous section.

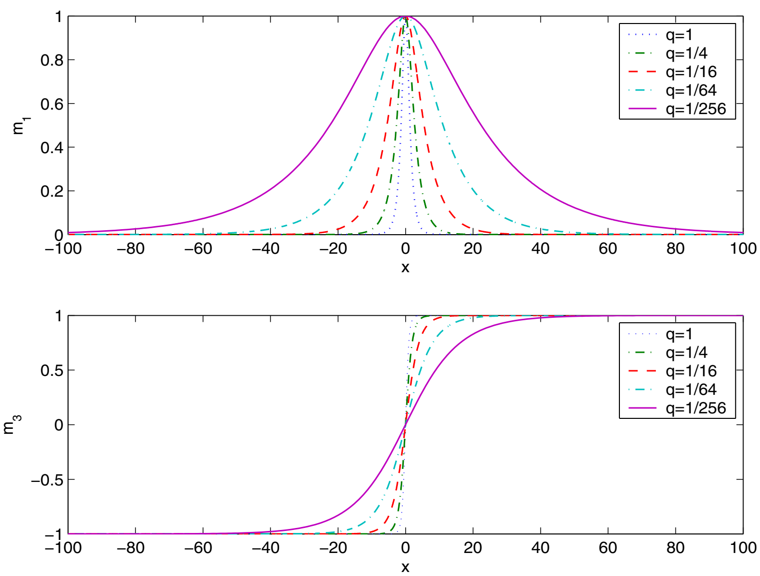

FIG. 2. *Néel wall profiles for several values of q.*

6. Conclusion. We have presented a new model for the analysis of one-dimensional walls in double layers. Using this new model, we have studied the structure of Néel walls and obtained the core length of the wall, the optimal energy scaling, and the structure of the minimizers. The main observation is that in a symmetric double layer the Néel wall no longer has a long logarithmic tail. The wall profile becomes local and similar to the classic Landau–Lifshitz wall. Thus, the range of nonlocal interactions is considerably reduced. We have implemented a truncated Newton method for energy minimization, and illustrated all the results numerically. In our simulations

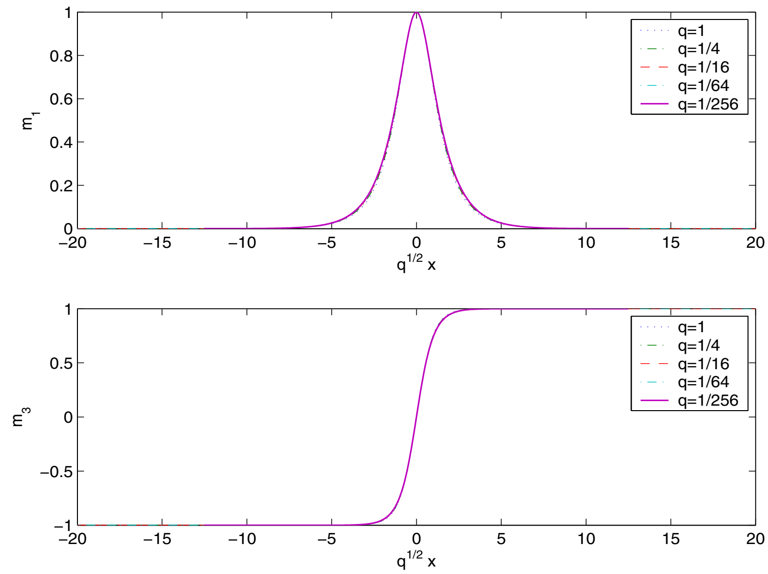

FIG. 3. *Néel wall profiles for several values of q. The abscissa has been rescaled to illustrate that the core length scales like $\sqrt{q}$.*

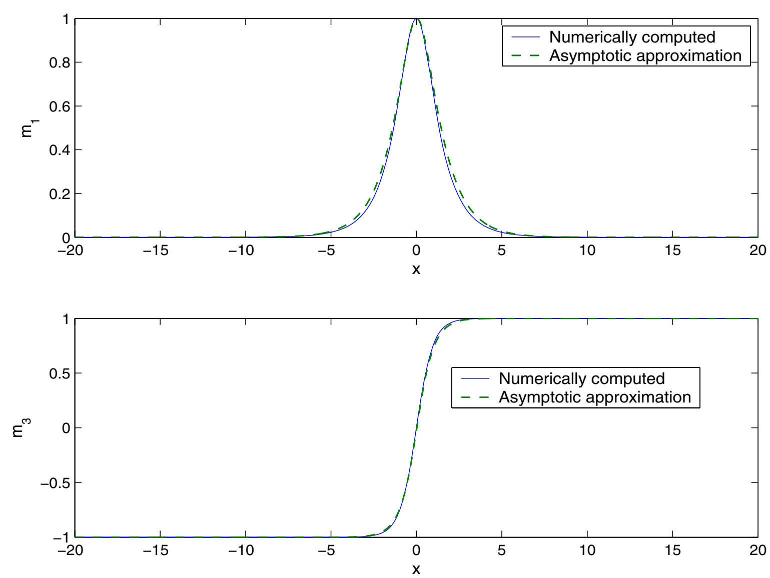

FIG. 4. *Comparison between the computed limiting profile and the asymptotic approximation obtained in section* 2.

we have managed to accurately capture the energy scaling, the core length, and the structure of the wall.

Appendix A. One-dimensional model for double layers. In this section we derive the model used in this article, starting from the Landau–Lifshitz energy functional.

TABLE 1

Minimum energy as a function of q. The energy is computed with the energy minimization algorithm described in section 5, and the energy scaling in q is obtained. We fixed the parameters $\delta = 1$ and $a = 10^{-1}$.

Energy scaling as $q \to 0$			
n	$q_n = 2^{-n}$	E_n	$\log \frac{E_{n-1}}{E_n} / \log 2$
0	1.000000E+00	0.413832547E+01	
1	5.000000E-01	0.294556828E+01	0.490501
2	2.500000E-01	0.209484869E+01	0.491699
3	1.250000E-01	0.148838645E+01	0.493096
4	6.250000E-02	0.105647543E+01	0.494489
5	3.125000E-02	0.749249198E+00	0.495741
6	1.562500E-02	0.530979818E+00	0.496788
7	7.812500E-03	0.376078916E+00	0.497621
8	3.906250E-03	0.266248579E+00	0.498261
9	1.953125E-04	0.188430720E+00	0.498739

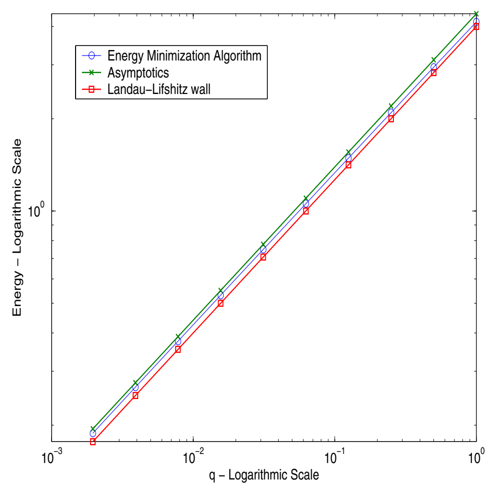

FIG. 5. *Comparison between the numerically computed energy, the optimal energy obtained in section 2, and the energy of the Landau–Lifshitz wall. The asymptotics give us an upper bound, while the Landau–Lifshitz wall provides us with a lower bound.*

We consider a double layer, infinite in both the x and y directions, and solve the magnetostatic equation in two dimensions. The stray field is $\mathbf{h}_s(x, z) = -\nabla\eta$, where

$$\eta = \nabla N * \mathbf{m} \tag{A.1}$$

is the magnetostatic potential, and $N(\mathbf{x}) = \frac{1}{2\pi}\log(|\mathbf{x}|)$, $\mathbf{x} = (x, z) \in \mathbb{R}^2$.

For the study on one-dimensional walls, we assume that $\mathbf{m}$ depends only on x. The double layer will be identified with the domain $\Omega = \mathbb{R} \times [-a - D_1, -a] \cup [a, a + D_2]$. In the bottom layer, we have $\mathbf{m} = (u_1, v_1, w_1)$, and in the top layer, $\mathbf{m} = (u_2, v_2, w_2)$.

Then,

$$
\eta(x,z) = \int_\Omega \partial_x N(x-s,z-t)u(s)\,ds + \int_\Omega \partial_z N(x-s,z-t)v(s)\,ds \tag{A.2}
$$

$$
\begin{aligned}
= \int_\Omega \partial_x N(x-s,z-t)u(s)\,ds &+ \int_{\mathbb{R}} \left(N(x-s,z+a+D_1) - N(x-s,z+a)\right) v_1(s)\,ds \\
&+ \int_{\mathbb{R}} \left(N(x-s,z-a) - N(x-s,z-a-D_2)\right) v_2(s)\,ds.
\end{aligned}
$$

The stray field energy is

$$
\begin{aligned}
\frac{2}{\mu_0 M_s^2} E &= \int_\Omega \nabla\eta\cdot\mathbf{m}\,dx\,dz = \int_\Omega u\partial_x\eta + v\partial_z\eta\,dx\,dz \\
&= \int_{\mathbb{R}} u_1(x)\int_{-a-D_1}^{-a} \partial_x\eta(x,z)\,dz\,dx + \int_{\mathbb{R}} u_2(x)\int_a^{a+D_2} \partial_x\eta(x,z)\,dz\,dx \\
&+ \int_{\mathbb{R}} v_1(x)\left(\eta(x,-a) - \eta(x,-a-D_1)\right)dx + \int_{\mathbb{R}} v_2(x)\left(\eta(x,a+D_2) - \eta(x,a)\right)dx.
\end{aligned} \tag{A.3}
$$

We can easily compute the derivative of η w.r.t. x:

$$
\begin{aligned}
\partial_x\eta(x,z) = \int_\Omega \partial_{xx} N(x-s,z-t)u(s)\,ds \\
&+ \int_{\mathbb{R}} \left(\partial_x N(x-s,z+a+D_1) - \partial_x N(x-s,z+a)\right) v_1(s)\,ds \\
&+ \int_{\mathbb{R}} \left(\partial_x N(x-s,z-a) - \partial_x N(x-s,z-a-D_2)\right) v_2(s)\,ds.
\end{aligned} \tag{A.4}
$$

Since $\Delta N = \delta$, we get that $\partial_{xx}N(x-s,z-t) = \delta_{(x,z)} - \partial_{zz}N(x-s,z-t)$. Substituting this,

$$
\begin{aligned}
\partial_x\eta(x,z) &= u(x) - \int_\Omega \partial_{zz} N(x-s,z-t)u(s)\,ds \\
&+ \int_{\mathbb{R}} \left(\partial_x N(x-s,z+a+D_1) - \partial_x N(x-s,z+a)\right) v_1(s)\,ds \\
&+ \int_{\mathbb{R}} \left(\partial_x N(x-s,z-a) - \partial_x N(x-s,z-a-D_2)\right) v_2(s)\,ds \\
&= u(x) - \int_{\mathbb{R}} \left(\partial_z N(x-s,z+a+D_1) - \partial_z N(x-s,z+a)\right) u_1(s)\,ds \\
&- \int_{\mathbb{R}} \left(\partial_z N(x-s,z-a) - \partial_z N(x-s,z-a-D_2)\right) u_2(s)\,ds \\
&+ \int_{\mathbb{R}} \left(\partial_x N(x-s,z+a+D_1) - \partial_x N(x-s,z+a)\right) v_1(s)\,ds \\
&+ \int_{\mathbb{R}} \left(\partial_x N(x-s,z-a) - \partial_x N(x-s,z-a-D_2)\right) v_2(s)\,ds.
\end{aligned} \tag{A.5}
$$

Now we compute the energy step by step:

(A.6)

$$\int_{\mathbb{R}} u_1(x) \int_{-a-D_1}^{-a} \partial_x \eta(x,z)\, dz\, dx = D_1 \int_{\mathbb{R}} u_1^2(x)\, dx - \int_{\mathbb{R}} u_1(x) \int_{\mathbb{R}} u_1(s)(N(x-s,D_1)$$

$$-2N(x-s,0) + N(x-s,-D_1))ds\, dx$$

$$-\int_{\mathbb{R}} u_1(x) \int_{\mathbb{R}} u_2(s)\big(N(x-s,-2a) - N(x-s,-2a-D_1)$$

$$-N(x-s,-2a-D_2) + N(x-s,-2a-D_1-D_2)\big)ds\, dx$$

$$+\frac{1}{2\pi} \int_{\mathbb{R}} u_1(x) \int_{\mathbb{R}} v_2(s)\Bigg(\arctan\left(\frac{2a+D_1}{x-s}\right) - \arctan\left(\frac{2a}{x-s}\right)$$

$$- \arctan\left(\frac{2a+D_1+D_2}{x-s}\right) + \arctan\left(\frac{2a+D_2}{x-s}\right)\Bigg) ds\, dx$$

$$= D_1 \int_{\mathbb{R}} u_1^2\, dx - D_1 \int_{\mathbb{R}} u_1\left(u_1 * \Gamma_{D_1}\right) dx + \frac{D_1 D_2}{2} \int_{\mathbb{R}} u_1\left(u_2 * \Theta_{a,D_1,D_2}\right) dx$$

$$+\frac{D_1 D_2}{2} \int_{\mathbb{R}} u_1\left(v_2 * \Psi_{a,D_1,D_2}\right) dx,$$

where we have defined

(A.7)

$$\Gamma_{D_i}(x) = \frac{1}{2\pi D_i} \log\left(1 + \frac{D_i^2}{x^2}\right), \quad i = 1,2,$$

$$\Theta_{a,D_1,D_2}(x) = \frac{1}{2D_1D_2\pi}\left(\log\left(\frac{x^2+(2a+D_1)^2}{x^2+(2a+D_1+D_2)^2}\right) - \log\left(\frac{x^2+4a^2}{x^2+(2a+D_2)^2}\right)\right),$$

$$\Psi_{a,D_1,D_2}(x) = \frac{1}{D_1D_2\pi}\Bigg(\arctan\left(\frac{2a+D_1}{x-s}\right) - \arctan\left(\frac{2a}{x-s}\right)$$

$$- \arctan\left(\frac{2a+D_1+D_2}{x-s}\right) + \arctan\left(\frac{2a+D_2}{x-s}\right)\Bigg), \tag{A.8}$$

$$\int_{\mathbb{R}} u_2(x) \int_{a}^{a+D_2} \partial_x \eta(x,z)\, dz\, dx = D_2 \int_{\mathbb{R}} u_2^2\, dx - D_2 \int_{\mathbb{R}} u_2\left(u_2 * \Gamma_{D_2}\right) dx \tag{A.9}$$

$$+ \frac{D_1D_2}{2} \int_{\mathbb{R}} u_2\left(u_1 * \Theta_{a,D_1,D_2}\right) dx - \frac{D_1D_2}{2} \int_{\mathbb{R}} u_2\left(v_1 * \Psi_{a,D_1,D_2}\right) dx.$$

Now

$$
\begin{aligned}
&\eta(x,-a)-\eta(x,-a-D_1)\\
&\quad=\int_{\mathbb{R}} u_1(s)\int_{-a-D_1}^{-a}\left(\partial_x N(x-s,-a-t)-\partial_x N(x-s,-a-D_1-t)\right)dt\,ds\\
&\qquad+\int_{\mathbb{R}} u_2(s)\int_{a}^{a+D_2}\left(\partial_x N(x-s,-a-t)-\partial_x N(x-s,-a-D_1-t)\right)dt\,ds\\
&\qquad+\int_{\mathbb{R}}\left(N(x-s,D_1)-2N(x-s,0)+N(x-s,-D_1)\right)v_1(s)\,ds\\
&\qquad+\int_{\mathbb{R}}\big(N(x-s,-2a)-N(x-s,-2a-D_2)\\
&\qquad\qquad-N(x-s,-2a-D_1)+N(x-s,-2a-D_1-D_2)\big)v_2(s)\,ds\\
&\quad=\frac{D_1D_2}{2}u_2*\Psi_{a,D_1,D_2}+D_1v_1*\Gamma_{D_1}-\frac{D_1D_2}{2}v_2*\Theta_{a,D_1,D_2} \qquad \text{(A.10)}
\end{aligned}
$$

and

$$
\begin{aligned}
&\eta(x,a+D_2)-\eta(x,a)\\
&\quad=\int_{\mathbb{R}} u_2(s)\int_{a}^{a+D_2}\left(\partial_x N(x-s,a+D_2-t)-\partial_x N(x-s,a-t)\right)dt\,ds\\
&\qquad+\int_{\mathbb{R}} u_1(s)\int_{-a-D_1}^{-a}\left(\partial_x N(x-s,a+D_2-t)-\partial_x N(x-s,a-t)\right)dt\,ds\\
&\qquad+\int_{\mathbb{R}}\big(N(x-s,2a+D_1+D_2)-N(x-s,2a+D_2)\\
&\qquad\qquad-N(x-s,2a+D_1)+N(x-s,2a)\big)v_1(s)\,ds\\
&\qquad+\int_{\mathbb{R}}\big(N(x-s,D_2)-2N(x-s,0)+N(x-s,-D_2)\big)v_2(s)\,ds\\
&\quad=-\frac{D_1D_2}{2}u_1*\Psi_{a,D_1,D_2}-\frac{D_1D_2}{2}v_1*\Theta_{a,D_1,D_2}+D_2v_2*\Gamma_{D_2}. \qquad \text{(A.11)}
\end{aligned}
$$

Assembling all this, we get the stray field energy:

$$
\begin{aligned}
\frac{2}{\mu_0M_s^2}E_s&=D_1\int_{\mathbb{R}}u_1^2\,dx-D_1\int_{\mathbb{R}}u_1\left(u_1*\Gamma_{D_1}\right)dx+D_1\int_{\mathbb{R}}v_1\left(v_1*\Gamma_{D_1}\right)dx\\
&\quad+D_2\int_{\mathbb{R}}u_2^2\,dx-D_2\int_{\mathbb{R}}u_2\left(u_2*\Gamma_{D_2}\right)dx+D_2\int_{\mathbb{R}}v_2\left(v_2*\Gamma_{D_2}\right)dx\\
&\quad+D_1D_2\int_{\mathbb{R}}u_1\left(u_2*\Theta_{a,D_1,D_2}\right)-v_1\left(v_2*\Theta_{a,D_1,D_2}\right)dx\\
&\quad+D_1D_2\int_{\mathbb{R}}u_1\left(v_2*\Psi_{a,D_1,D_2}\right)-v_1\left(u_2*\Psi_{a,D_1,D_2}\right)dx. \qquad \text{(A.12)}
\end{aligned}
$$

In order to write this in Fourier space, we need the Fourier transform of the convolution kernels. We start with the following:

$$\begin{aligned}\int_{\mathbb{R}} \log\left(\frac{x^2+\alpha^2}{x^2+\beta^2}\right) e^{-2\pi i\xi x}\,dx &= \int_{\mathbb{R}} \log\left(1+\frac{\alpha^2-\beta^2}{x^2+\beta^2}\right) e^{-2\pi i\xi x}\,dx \\ &= \frac{\beta^2-\alpha^2}{2\pi i\xi}\int_{\mathbb{R}} \frac{1}{1+\frac{\alpha^2-\beta^2}{x^2+\beta^2}}\,\frac{2x}{(x^2+\beta^2)^2} e^{-2\pi i\xi x}\,dx \\ &= \frac{\beta^2-\alpha^2}{2\pi i\xi}\int_{\mathbb{R}} \frac{2x}{(x^2+\alpha^2)(x^2+\beta^2)} e^{-2\pi i\xi x}\,dx.\end{aligned} \tag{A.13}$$

Using residue theory, we get that

$$\begin{aligned}\int_{\mathbb{R}} \frac{2x}{(x^2+\alpha^2)(x^2+\beta^2)} e^{-2\pi i\xi x}\,dx &= 2\pi i(\mathrm{Res}\,(f,i\alpha)+\mathrm{Res}\,(f,i\beta)) \\ &= 2\pi i\left(\frac{2i\beta}{2i\beta(\alpha^2-\beta^2)}e^{2\pi\beta\xi}+\frac{2i\alpha}{2i\alpha(\beta^2-\alpha^2)}e^{2\pi\alpha\xi}\right)\end{aligned} \tag{A.14}$$

for $\xi<0$. When we put it all together, we get

$$\int_{\mathbb{R}} \log\left(\frac{x^2+\alpha^2}{x^2+\beta^2}\right) e^{-2\pi i\xi x}\,dx = \frac{e^{-2\pi\beta|\xi|}-e^{-2\pi\alpha|\xi|}}{|\xi|}. \tag{A.15}$$

Therefore

$$\frac{1}{2\pi}\int_{\mathbb{R}} \log\left(1+\frac{D_j^2}{x^2}\right) e^{-2\pi i\xi x}\,dx = \frac{1-e^{-2\pi D_j|\xi|}}{2\pi|\xi|}, \quad j=1,2, \tag{A.16}$$

and

$$\begin{aligned}\frac{1}{2\pi}\int_{\mathbb{R}} \left(\log\left(\frac{x^2+4a^2}{x^2+(2a+D_2)^2}\right)-\log\left(\frac{x^2+(2a+D_1)^2}{x^2+(2a+D_1+D_2)^2}\right)\right) e^{-2\pi i\xi x}\,dx \\ = -e^{-4\pi a|\xi|}\frac{(1-e^{-2\pi D_1|\xi|})(1-e^{-2\pi D_2|\xi|})}{2\pi|\xi|}.\end{aligned} \tag{A.17}$$

Finally,

$$\begin{aligned}\frac{1}{\pi}\int_{\mathbb{R}} e^{-2\pi i\xi x}\arctan\left(\frac{\alpha}{x}\right)dx &= -\frac{2i}{\pi}\int_0^\infty \sin(2\pi\xi x)\arctan\left(\frac{\alpha}{x}\right)dx \\ &= -\frac{2i}{\pi}\left(-\frac{1}{2\pi\xi}\cos(2\pi\xi x)\arctan\left(\frac{\alpha}{x}\right)\Big|_0^\infty - \frac{\alpha}{2\pi\xi}\int_0^\infty \cos(2\pi\xi x)\frac{1}{\alpha^2+x^2}\,dx\right) \\ &= -i\frac{1-e^{-2\pi|\xi|\alpha}}{2\pi\xi}.\end{aligned} \tag{A.18}$$

Therefore

$$\begin{aligned}\frac{1}{\pi}\int_{\mathbb{R}} e^{-2\pi i\xi x}\Bigg(\arctan\left(\frac{2a+D_1}{x}\right)-\arctan\left(\frac{2a}{x}\right) \\ -\arctan\left(\frac{2a+D_1+D_2}{x}\right)+\arctan\left(\frac{2a+D_2}{x}\right)\Bigg)dx \\ = -ie^{-4\pi a|\xi|}\frac{(1-e^{-2\pi|\xi|D_1})(1-e^{-2\pi|\xi|D_2})}{2\pi\xi}.\end{aligned} \tag{A.19}$$

Thus, the stray field energy can be written in Fourier space as

(A.20)
$$\frac{2}{\mu_0 M_s^2}E_s = D_1\int_{\mathbb{R}} \widehat{u_1}^2(\xi)\left(1-\frac{1-e^{-2\pi D_1|\xi|}}{2\pi D_1|\xi|}\right)d\xi + D_1\int_{\mathbb{R}} \widehat{v_1}^2(\xi)\frac{1-e^{-2\pi D_1|\xi|}}{2\pi D_1|\xi|}\,d\xi$$
$$+D_2\int_{\mathbb{R}} \widehat{u_2}^2(\xi)\left(1-\frac{1-e^{-2\pi D_2|\xi|}}{2\pi D_2|\xi|}\right)d\xi + D_2\int_{\mathbb{R}} \widehat{v_2}^2(\xi)\frac{1-e^{-2\pi D_2|\xi|}}{2\pi D_2|\xi|}\,d\xi$$
$$+\int_{\mathbb{R}}(\widehat{u_1}(\xi)\overline{\widehat{u_2}}(\xi)-\widehat{v_1}(\xi)\overline{\widehat{v_2}}(\xi))e^{-4\pi a|\xi|}\,\frac{(1-e^{-2\pi D_1|\xi|})(1-e^{-2\pi D_2|\xi|})}{2\pi|\xi|}\,d\xi$$
$$-i\int_{\mathbb{R}}\left(\widehat{v_1}(\xi)\overline{\widehat{u_2}}(\xi)-\widehat{u_1}(\xi)\overline{\widehat{v_2}}(\xi)\right)e^{-4a\pi|\xi|}\,\frac{(1-e^{-2\pi D_1|\xi|})(1-e^{-2\pi D_2|\xi|})}{2\pi\xi}\,d\xi.$$

Note that the interaction between the layers decays exponentially with the spacer distance.

In this one-dimensional setting, the Landau–Lifshitz energy for a double layer reduces to

(A.21)
$$F[\mathbf{m}_1,\mathbf{m}_2] = \frac{K_u D_1}{2}\int_{\mathbb{R}}\left(u_1^2+v_1^2\right)dx + \frac{AD_1}{2}\int_{\mathbb{R}}|\mathbf{m}_1'|^2\,dx$$
$$+\frac{D_1\mu_0M_s^2}{2}\int_{\mathbb{R}}u_1^2\,dx - \frac{D_1\mu_0M_s^2}{2}\int_{\mathbb{R}}u_1\left(\Gamma_{D_1}*u_1\right)dx + \frac{D_1\mu_0M_s^2}{2}\int_{\mathbb{R}}v_1\left(\Gamma_{D_1}*v_1\right)dx$$
$$+\frac{K_u D_2}{2}\int_{\mathbb{R}}\left(u_2^2+v_2^2\right)dx + \frac{AD_2}{2}\int_{\mathbb{R}}|\mathbf{m}_2'|^2\,dx$$
$$+\frac{D_2\mu_0M_s^2}{2}\int_{\mathbb{R}}u_2^2\,dx - \frac{D_2\mu_0M_s^2}{2}\int_{\mathbb{R}}u_2\left(\Gamma_{D_2}*u_2\right)dx + \frac{D_2\mu_0M_s^2}{2}\int_{\mathbb{R}}v_2\left(\Gamma_{D_2}*v_2\right)dx$$
$$+\frac{D_1D_2\mu_0M_s^2}{2}\int_{\mathbb{R}}u_1\left(u_2*\Theta_{a,D_1,D_2}\right)-v_1\left(v_2*\Theta_{a,D_1,D_2}\right)dx$$
$$+\frac{D_1D_2\mu_0M_s^2}{2}\int_{\mathbb{R}}v_1\left(u_2*\Psi_{a,D_1,D_2}\right)-u_1\left(v_2*\Psi_{a,D_1,D_2}\right)dx,$$

where

$$\Gamma_i(x) = \frac{1}{2\pi D_i}\log\left(1+\frac{D_i^2}{x^2}\right),\quad i=1,2,$$

$$\Theta_{a,D_1,D_2}(x) = \frac{1}{2D_1D_2\pi}\left(\log\left(\frac{x^2+(2a+D_1)^2}{x^2+(2a+D_1+D_2)^2}\right)-\log\left(\frac{x^2+4a^2}{x^2+(2a+D_2)^2}\right)\right),$$

$$\Psi_{a,D_1,D_2}(x) = \frac{1}{D_1D_2\pi}\left(\arctan\left(\frac{2a+D_1}{x-s}\right)-\arctan\left(\frac{2a}{x-s}\right)\right.$$

(A.22)
$$\left.-\arctan\left(\frac{2a+D_1+D_2}{x-s}\right)+\arctan\left(\frac{2a+D_2}{x-s}\right)\right)$$

and in Fourier space

$$\widehat{\Gamma}_{D_j}(\xi) = \frac{1-e^{-2\pi D_j|\xi|}}{2\pi D_j|\xi|}, \quad j=1,2,$$
$$\widehat{\Theta}_{a,D_1,D_2}(\xi) = e^{-4\pi a|\xi|}\frac{\left(1-e^{-2\pi D_1|\xi|}\right)\left(1-e^{-2\pi D_2|\xi|}\right)}{2\pi D_1 D_2|\xi|},$$
$$\widehat{\Psi}_{a,D_1,D_2}(\xi) = ie^{-4\pi a|\xi|}\frac{\left(1-e^{-2\pi D_1|\xi|}\right)\left(1-e^{-2\pi D_2|\xi|}\right)}{2\pi D_1 D_2\xi}. \tag{A.23}$$

To write the energy in dimensionless variables, we define $x = lx'$, $a = l\alpha$, $D_1 = l\delta_1$, and $D_2 = l\delta_2$, where $l = \sqrt{A/(\mu_0 M_s^2)}$. Define also $q = K_u/(\mu_0 M_s^2)$. Performing this change of variables and dropping the prime in x', we obtain

$$\begin{aligned}
\frac{1}{D_1\sqrt{\mu_0 M_s^2 A}}F[\mathbf{m}_1,\mathbf{m}_2] = {} & \frac{q}{2}\int_{\mathbb{R}}\left(u_1^2+v_1^2\right)dx + \frac{1}{2}\int_{\mathbb{R}}|\mathbf{m}_1'|^2\,dx \\
& +\frac{1}{2}\int_{\mathbb{R}}u_1^2\,dx - \frac{1}{2}\int_{\mathbb{R}}u_1\left(\Gamma_{\delta_1}*u_1\right)dx \\
& +\frac{1}{2}\int_{\mathbb{R}}v_1\left(\Gamma_{\delta_1}*v_1\right)dx + \frac{q\delta_2}{2\delta_1}\int_{\mathbb{R}}\left(u_2^2+v_2^2\right)dx \\
& +\frac{\delta_2}{2\delta_1}\int_{\mathbb{R}}|\mathbf{m}_2'|^2\,dx + \frac{\delta_2}{2\delta_1}\int_{\mathbb{R}}u_2^2\,dx \\
& -\frac{\delta_2}{2\delta_1}\int_{\mathbb{R}}u_2\left(\Gamma_{\delta_2}*u_2\right)dx + \frac{\delta_2}{2\delta_1}\int_{\mathbb{R}}v_2\left(\Gamma_{\delta_2}*v_2\right)dx \\
& +\frac{\delta_2}{2}\int_{\mathbb{R}}u_1\left(u_2*\Theta_{\alpha,\delta_1,\delta_2}\right) - v_1\left(v_2*\Theta_{\alpha,\delta_1,\delta_2}\right)dx \\
& +\frac{\delta_2}{2}\int_{\mathbb{R}}v_1\left(u_2*\Psi_{\alpha,\delta_1,\delta_2}\right) - u_1\left(v_2*\Psi_{\alpha,\delta_1,\delta_2}\right)dx.
\end{aligned} \tag{A.24}$$

Appendix B. Validity range for the upper bound. In order to estimate the value of q_0 in (2.18), we need to study the stray field (2.17). Define

$$\eta = \frac{2\delta|\xi|\sqrt{q}}{\pi} \tag{B.1}$$

and

$$\beta = \frac{\alpha}{\delta}. \tag{B.2}$$

We need to study the Taylor series of

$$\phi(\eta) = 1 - \frac{1-e^{-\eta}}{\eta} - \frac{1}{2}e^{-2\beta\eta}\frac{(1-e^{-\eta})^2}{\eta}. \tag{B.3}$$

Using the Taylor polynomials of $e^{-\eta}$ and $e^{-2\beta\eta}$, we obtain

$$\begin{aligned}
\phi(\eta) = \left(\frac{1}{3}+\beta\right)\eta^2 + \eta^3\Bigg(&\frac{e^{-\eta_1}}{4!} - \beta^2 e^{-2\beta\eta_3} - \beta e^{-2\beta\eta_4} \\
&- \frac{e^{-2\beta\eta}}{2}\left(\frac{1}{4}+\frac{1}{3}e^{-\eta_2} - \frac{\eta}{3!}e^{-\eta_2} + \frac{\eta^2}{36}e^{-2\eta_2}\right)\Bigg),
\end{aligned} \tag{B.4}$$

where $\eta_k \in [0, \eta]$ for $k = 1, 2, 3, 4$. Using (B.4), (B.1), and (B.2) in (2.17), we obtain

$$E_s \leq \frac{2\delta\sqrt{q}}{3}\left(\frac{\delta}{3}+\alpha\right) + \frac{8\delta^3 q}{\pi^3}\left(\frac{1}{3}+\frac{\alpha^2}{\delta^2}+\frac{\alpha}{\delta}\right)\int |\xi|^3 \mathrm{sech}^2(\xi)\, d\xi + \frac{4\delta^4 q^{3/2}}{3\pi^4}\int |\xi|^4 \mathrm{sech}^2(\xi)\, d\xi + \frac{4\delta^5 q^2}{9\pi^5}\int |\xi|^5 \mathrm{sech}^2(\xi)\, d\xi. \tag{B.5}$$

Estimate (2.20) holds for

$$q_0 \leq \min\left\{ M, \frac{4}{9}\left(\frac{\delta}{3}+\alpha\right)^2 \left[\frac{8}{\pi^3}\left(\frac{\delta^2}{3}+\alpha^2+\delta\alpha\right)\int |\xi|^3 \mathrm{sech}^2(\xi)\, d\xi + \frac{4\delta^3 M^{1/2}}{3\pi^4}\int |\xi|^4 \mathrm{sech}^2(\xi)\, d\xi + \frac{4\delta^4 M^{3/2}}{9\pi^5}\int |\xi|^5 \mathrm{sech}^2(\xi)\, d\xi\right]^{-2}\right\}, \tag{B.6}$$

where $M > 0$ is arbitrary.

Note that as $\alpha \to \infty$, $q_0 \to 0$. This is consistent with the fact that as $\alpha \to \infty$, the layers are decoupled, and we recover the Néel wall energy for a single layer, for which the upper bound is not (2.20) but (1.7).

Acknowledgment. The author wishes to thank the anonymous reviewer. His/her comments helped improve considerably the presentation of the results in this article.

REFERENCES

[1] A. Aharoni, *Energy of one dimensional domain walls in ferromagnetic films*, J. Appl. Phys., 37 (1966), pp. 3271–3279.

[2] L. Ahlfors, *Complex Analysis*, 3rd ed., McGraw-Hill, New York, 1979.

[3] G. Carbou, *Thin layers in micromagnetism*, Math. Models Methods Appl. Sci., 11 (2001), pp. 1529–1546.

[4] R. Choksi and R. V. Kohn, *Bounds on the micromagnetic energy of a uniaxial ferromagnet*, Comm. Pure Appl. Math., 51 (1998), pp. 259–289.

[5] R. Choksi, R. V. Kohn, and F. Otto, *Domain branching in uniaxial ferromagnets: A scaling law for the minimum energy*, Comm. Math. Phys., 201 (1999), pp. 61–79.

[6] C. J. García-Cervera, *Magnetic Domains and Magnetic Domain Walls*, Ph.D. thesis, Courant Institute of Mathematical Sciences, New York University, New York, 1999.

[7] C. J. García-Cervera, *One-dimensional magnetic domain walls*, European J. Appl. Math., 15 (2004), pp. 451–486.

[8] C. J. García-Cervera and W. E, *Effective dynamics in thin ferromagnetic films*, J. Appl. Phys., 90 (2000), pp. 370–374.

[9] G. Gioia and R. D. James, *Micromagnetics of very thin films*, Proc. Roy. Soc. London Ser. A, 453 (1997), pp. 213–223.

[10] A. Hubert and R. Schäfer, *Magnetic Domains: The Analysis of Magnetic Microstructures*, Springer-Verlag, Berlin, Heidelberg, New York, 1998.

[11] R. V. Kohn and V. V. Slastikov, *Effective dynamics for ferromagnetic thin films: A rigorous justification*, Proc. Roy. Soc. London Ser. A, 461 (2005), pp. 143–154.

[12] L. Landau and E. Lifshitz, *On the theory of the dispersion of magnetic permeability in ferromagnetic bodies*, Physikalische Zeitschrift der Sowjetunion, 8 (1935), pp. 153–169.

[13] G. Dal Maso, *An introduction to Γ-Convergence*, Progr. Nonlinear Differential Equations Appl. 8, Birkhäuser Boston, Cambridge, MA, 1993.

[14] S. Middelhoek, *Domain wall structures in magnetic double films*, J. Appl. Phys., 37 (1966), pp. 1276–1282.

[15] J. Nocedal and S. Wright, *Numerical Optimization*, Springer Ser. Oper. Res., Springer-Verlag, New York, 1999.

[16] F. Otto, *Cross-over in scaling laws: A simple example from micromagnetics*, in Proceedings of the International Congress of Mathematicians, Vol. 3, Higher Education Press, Beijing, 2002, pp. 829–838.

[17] I. Puchalska and H. Niedoba, *Magnetization process in permalloy multilayer films*, IEEE Trans. Magn., 27 (1991), pp. 3579–3587.

[18] A. De Simone, R. V. Kohn, S. Müller, and F. Otto, *Magnetic microstructures—A paradigm of multiscale problems*, in Proceedings of the ICIAM, Edinburgh, 1999, Oxford University Press, Oxford, UK, 2000, pp. 175–190.

[19] J. C. Slonczewski, *Theory of domain-wall motion in magnetic films and platelets*, J. Appl. Phys., 44 (1973), pp. 1759–1770.

[20] J. C. Slonczewski, *Theory of bloch-line and bloch-wall motion*, J. Appl. Phys., 45 (1974), pp. 2705–2715.

[21] W. P. Ziemer, *Weakly Differentiable Functions. Sobolev Spaces and Functions of Bounded Variation*, Grad. Texts in Math. 120, Springer-Verlag, New York, 1989.